LETTER

doi:10.1038/nature11893

Porous materials with optimal adsorption thermodynamics and kinetics for CO_2 separation

Patrick Nugent[1]*, Youssef Belmabkhout[2]*, Stephen D. Burd[1], Amy J. Cairns[2], Ryan Luebke[2], Katherine Forrest[1], Tony Pham[1], Shengqian Ma[1], Brian Space[1], Lukasz Wojtas[1], Mohamed Eddaoudi[1,2] & Michael J. Zaworotko[1]

The energy costs associated with the separation and purification of industrial commodities, such as gases, fine chemicals and fresh water, currently represent around 15 per cent of global energy production, and the demand for such commodities is projected to triple by 2050 (ref. 1). The challenge of developing effective separation and purification technologies that have much smaller energy footprints is greater for carbon dioxide (CO_2) than for other gases; in addition to its involvement in climate change, CO_2 is an impurity in natural gas, biogas (natural gas produced from biomass), syngas (CO/H_2, the main source of hydrogen in refineries) and many other gas streams. In the context of porous crystalline materials that can exploit both equilibrium and kinetic selectivity, size selectivity and targeted molecular recognition are attractive characteristics for CO_2 separation and capture, as exemplified by zeolites 5A and 13X (ref. 2), as well as metal–organic materials (MOMs)[3–9]. Here we report that a crystal engineering[7] or reticular chemistry[5,9] strategy that controls pore functionality and size in a series of MOMs with coordinately saturated metal centres and periodically arrayed hexafluorosilicate (SiF_6^{2-}) anions enables a 'sweet spot' of kinetics and thermodynamics that offers high volumetric uptake at low CO_2 partial pressure (less than 0.15 bar). Most importantly, such MOMs offer an unprecedented CO_2 sorption selectivity over N_2, H_2 and CH_4, even in the presence of moisture. These MOMs are therefore relevant to CO_2 separation in the context of post-combustion (flue gas, CO_2/N_2), pre-combustion (shifted synthesis gas stream, CO_2/H_2) and natural gas upgrading (natural gas clean-up, CO_2/CH_4).

Porous materials with unsaturated metal centres (UMCs)[10] or organic amines that chemically interact with CO_2 enhance selectivity for CO_2 in the presence of other gases. However, there are drawbacks: high energy costs associated with activation, regeneration and recycling of the sorbent material, especially for amines[11]; competition with water vapour, especially for UMCs[12]; and selectivity tends to monotonically decrease with increased loading of sorbate. Consequently, there remains a need for sorbents with favourable CO_2 sorption kinetics and thermodynamics over a wide range of CO_2 loading that would permit efficient CO_2 capture with low regeneration costs. MOMs are attractive in this context because they are inherently modular—that is, they consist of metals or metal clusters ('nodes' or 'molecular building blocks') coordinated to multi-functional organic ligands ('linkers')—and they offer extra-large surface areas, up to 7,000 $m^2\,g^{-1}$ (ref. 6). However, although extra-large surface area facilitates high gravimetric uptake of gases at low temperature and/or high pressure, it is not necessarily conducive to efficient separations under practical conditions. Here we address how to optimize the thermodynamics and kinetics of gas adsorption through a class of MOMs that is amenable to crystal engineering or isoreticular chemistry in a manner that facilitates precise control over pore size and functionality: namely, 'pillared square grids', two-dimensional nets based on linked metal nodes that are pillared via SiF_6^{2-} anions ('SIFSIX') in the third dimension to form three-dimensional nets with primitive cubic topology[13].

$[Cu(4,4'\text{-bipyridine})_2(SiF_6)]_n$, a prototypal primitive-cubic net that remains one of the best sorbents for CH_4 as measured by volumetric uptake[14], exhibits highly selective CO_2 uptake versus both CH_4 and N_2 at 1 bar and 298 K (ref. 15). In the absence of UMCs or amine groups, we attributed this behaviour to favourable interactions between CO_2 and SIFSIX. This compound, which we call here SIFSIX-1-Cu, exhibits one-dimensional square channels (pore size 9.54 Å; here and throughout this Letter, pore sizes are given as diagonal dimensions) aligned by a periodic array of SIFSIX pillars, and is prototypical for a class of compounds that is amenable to pore-size tuning. In this Letter we report the synthesis, structure and sorption properties of three variants of SIFSIX-1-Cu with expanded and contracted pore sizes.

Reaction of 4,4′-dipyridylacetylene, dpa (ref. 16), with $CuSiF_6$ afforded purple rod-shaped crystals of $[Cu(dpa)_2(SiF_6)]_n$, which we refer to as SIFSIX-2-Cu (see Supplementary Information for synthetic and crystallographic details for this and other compounds reported here). SIFSIX-2-Cu forms the expected primitive-cubic net with square channels of pore dimensions 13.05 Å (Fig. 1a). The interpenetrated polymorph, SIFSIX-2-Cu-i (Fig. 1b), is composed of doubly interpenetrated nets that are isostructural to the nets in SIFSIX-2-Cu. The independent nets are staggered with respect to one another, affording 5.15 Å pores (Fig. 1b). The isoreticular MOM based on pyrazine (pyr) SIFSIX-3-Zn, $[Zn(pyr)_2(SiF_6)]_n$, was prepared according to published procedures[17] and is also a primitive-cubic net which encloses 3.84 Å channels (Fig. 1c). Pore sizes in this series therefore range from ultra-microporous to nanoporous. Bulk purity was confirmed using powder X-ray diffraction (PXRD) patterns (Supplementary Figs 1–3).

Activation of SIFSIX-2-Cu and SIFSIX-2-Cu-i (evacuation at 298 K for 12 h) afforded BET apparent surface areas of 3,140 and 735 $m^2\,g^{-1}$, respectively (corresponding Langmuir values, 3,370 and 821 $m^2\,g^{-1}$), from N_2 adsorption isotherms at 77 K. Micropore volumes are in good agreement with corresponding theoretical values (Supplementary Fig. 4 and Supplementary Table 3). SIFSIX-3-Zn adsorbs minimal amounts of N_2 at 77 K and thus its surface area (250 $m^2\,g^{-1}$) was determined from the CO_2 isotherm collected at 298 K (ref. 18).

Low-pressure CO_2, CH_4 and N_2 sorption data were collected at 298 K (Supplementary Fig. 5a, Table 1). SIFSIX-2-Cu exhibited CO_2 uptake of 41.4 $cm^3\,g^{-1}$ (equivalent to 1.84 mmol g^{-1} or 81.3 mg g^{-1}) at 298 K and 1 bar, but its denser polymorph, SIFSIX-2-Cu-i, exhibited substantially higher values of 121.2 $cm^3\,g^{-1}$ (5.41 mmol g^{-1}, 238 mg g^{-1}). Such behaviour has also been observed in the context of hydrogen adsorption[19]. A review of the literature reveals that the gravimetric CO_2 uptake of SIFSIX-2-Cu-i at 298 K and 1 bar is among the highest yet reported in the context of MOMs (for example, Mg-dobdc (ref. 10), Co-dobdc (ref. 10), MIL-101 (ref. 20), [Cu(Me-4py-trz-ia)] (ref. 21) and partially hydrated HKUST-1 (ref. 22)). Notably, the above-mentioned

[1]Department of Chemistry, University of South Florida, 4202 East Fowler Avenue, Tampa, Florida 33620, USA. [2]Advanced Membranes and Porous Materials Center, Division of Physical Sciences and Engineering, 4700 King Abdullah University of Science and Technology (KAUST), Thuwal 23955-6900, Saudi Arabia.
*These authors contributed equally to this work.

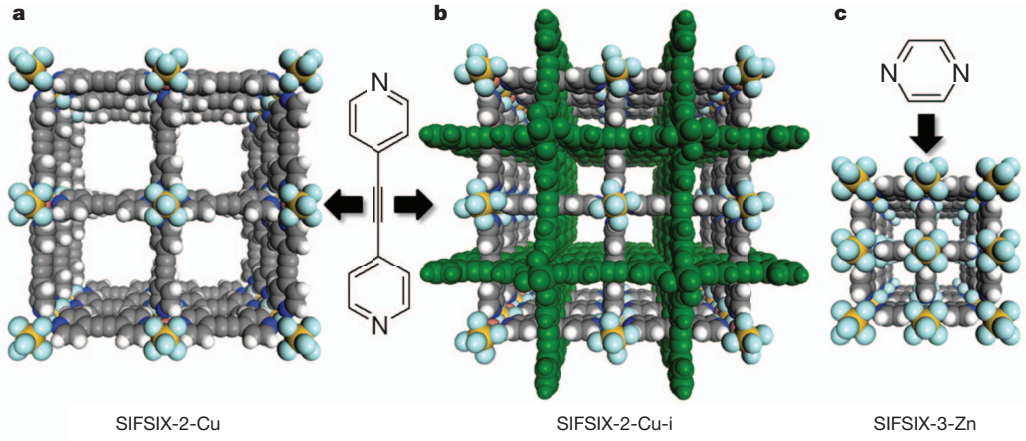

Figure 1 | The variable pore size channel structures of SIFSIX-2-Cu, SIFSIX-2-Cu-i and SIFSIX-3-Zn. **a**, SIFSIX-2-Cu; pore size 13.05 Å, BET apparent surface area (N_2 adsorption) 3,140 $m^2 g^{-1}$. **b**, SIFSIX-2-Cu-i; pore size 5.15 Å, BET apparent surface area (N_2 adsorption) 735 $m^2 g^{-1}$. **c**, SIFSIX-3-Zn; pore size 3.84 Å, apparent surface area (determined from CO_2 adsorption isotherm) 250 $m^2 g^{-1}$. Colour code: C (grey), N (blue), Si (yellow), F (light blue), H (white). All guest molecules are omitted for clarity. Note that the green net represents the interpenetrated net in SIFSIX-2-Cu-i. The nitrogen-containing linker present in SIFSIX-2-Cu and SIFSIX-2-Cu-i is 4,4′-dipyridylacetylene (dpa) whereas that in SIFSIX-3-Zn is pyrazine (pyr).

benchmark MOMs possess higher surface area, are less dense than SIFSIX-2-Cu-i and contain UMCs. Volumetric CO_2 uptake of SIFSIX-2-Cu-i at atmospheric pressure approaches that of Mg-dobdc (151 versus 163 v/v). Ideal adsorbed solution theory (IAST)[23] calculations indicate binary gas adsorption selectivity (Supplementary Fig. 5b) under practically relevant conditions (298 K; CH_4 and N_2 mole fractions equal to 0.5 and 0.9, respectively) to be dramatically higher for SIFSIX-2-Cu-i than SIFSIX-2-Cu for both CO_2/CH_4 (33 versus 5.3) and CO_2/N_2 (140 versus 13.7). These findings agree with the CO_2/CH_4 (51) and CO_2/N_2 (72) adsorption selectivity determined experimentally for SIFSIX-2-Cu-i using column breakthrough tests, a technique that determines the necessary time for a given volume of a gas to pass through a given sorbent bed column (Supplementary Fig. 6). To the best of our knowledge, the CO_2/CH_4 and CO_2/N_2 IAST selectivities exhibited by SIFSIX-2-Cu-i are the highest yet reported for a MOM without UMCs or amino groups. We attribute these observations to the enhanced isosteric heat of adsorption (Q_{st}) of SIFSIX-2-Cu-i versus SIFSIX-2-Cu (45% higher at minimum loading, 71.5% greater at 2.8 mmol g^{-1}, Supplementary Fig. 5c). This increase is presumably attributable to better overlap of attractive potential fields of opposite walls in the relatively narrower pores of SIFSIX-2-Cu-i. SIFSIX-2-Cu-i is particularly suitable for CO_2 separation from syngas, as shown by its selectivity (240) for CO_2 over H_2 in a CO_2/H_2:30/70 mixture, and as determined from column breakthrough experiments (Supplementary Fig. 6c).

The heart of pressure- and temperature-swing adsorption (PSA and TSA) processes for CO_2 removal is the adsorbent bed: a recent study projected that a CO_2/N_2 selectivity of >500 combined with a capacity of 2–4 mmol g^{-1} for a CO_2/N_2:10/90 mixture would be required for practical utility (Supplementary Fig. 7)[24]. Figure 2a and b presents the CO_2 adsorption isotherms of SIFSIX-2-Cu-i and SIFSIX-3-Zn, respectively, collected at sub-atmospheric pressures after activation at 298 K. Contraction of the pores led to a sharp increase in CO_2 uptake at low CO_2 loading, with nearly 11 wt% at 0.1 bar for SIFSIX-3-Zn versus 4.4 wt% at 0.1 bar for SIFSIX-2-Cu-i. Notably, the CO_2 uptake for SIFSIX-3-Zn reached saturation at relatively low pressures (~0.3 bar; Supplementary Fig. 8), whereas the isotherm for CO_2

Table 1 | Gas adsorption/CO_2 selectivity results and comparisons

Property		Compounds				
		SIFSIX-2-Cu	SIFSIX-2-Cu-i	SIFSIX-3-Zn	Mg-dobdc*	13X†
Pore size (Å)		13.05	5.15	3.84	10.8	10
Single-gas data						
Q_{st} for CO_2 at low CO_2 loading (kJ mol^{-1})		22	31.9	45	47–52	44–54
CO_2 uptake at 298 K at 0.1 bar/1 bar (mg g^{-1})		10/81.3	76/238	105/112	220/352	106/220
CO_2 uptake at 298 K at 0.1 bar/1 bar (cm^3 cm^{-3})		3/26	48/151	84/90	101/162	61/126
CH_4 uptake at 298 K at 1 bar (mg g^{-1})		6.2	7.5	12.6	17.8	4.2
N_2 uptake at 298 K at 1 bar (mg g^{-1})		4.9	4.2	6.4	NA	6.4
H_2 uptake at 298 K at 1 bar (mg g^{-1})		NM	0.2	1.37	NA	NA
Mixed-gas data						
CO_2 uptake at 298 K in CO_2/N_2:10/90 mixture at 1 bar (mg g^{-1})		8.4‡	70‡/55§	99.9‡/104.4¶	NA	NA
CO_2 uptake at 298 K in CO_2/CH_4:50/50 mixture at 1 bar (mg g^{-1})		42.8‡	183‡/138§	108‡/110¶	NA	NA
CO_2 uptake at 298 K in CO_2/H_2:30/70 mixture at 1 bar (mg g^{-1})		NM	85§	112 ‖	NA	NA
Selectivity at 1 bar	CO_2/N_2	13.7‡	140‡/72§	1,818‡/1,700¶	NA	420‡
Selectivity at 1 bar	CO_2/CH_4	5.3‡	33‡/51§	231‡/350¶	137‡	103‡
Selectivity at 1 bar	CO_2/H_2	NM	240§	>1,800	800*	NA

NA, not available; NM, not measured.
* Ref. 29 (313 K data).
† Ref. 26 (298 K data).
‡ IAST.
§ Breakthrough experiments.
‖ Mixture gravimetric (G) experiment.
¶ Mixture gravimetric-densimetric gas analysis (GDGA) experiment.

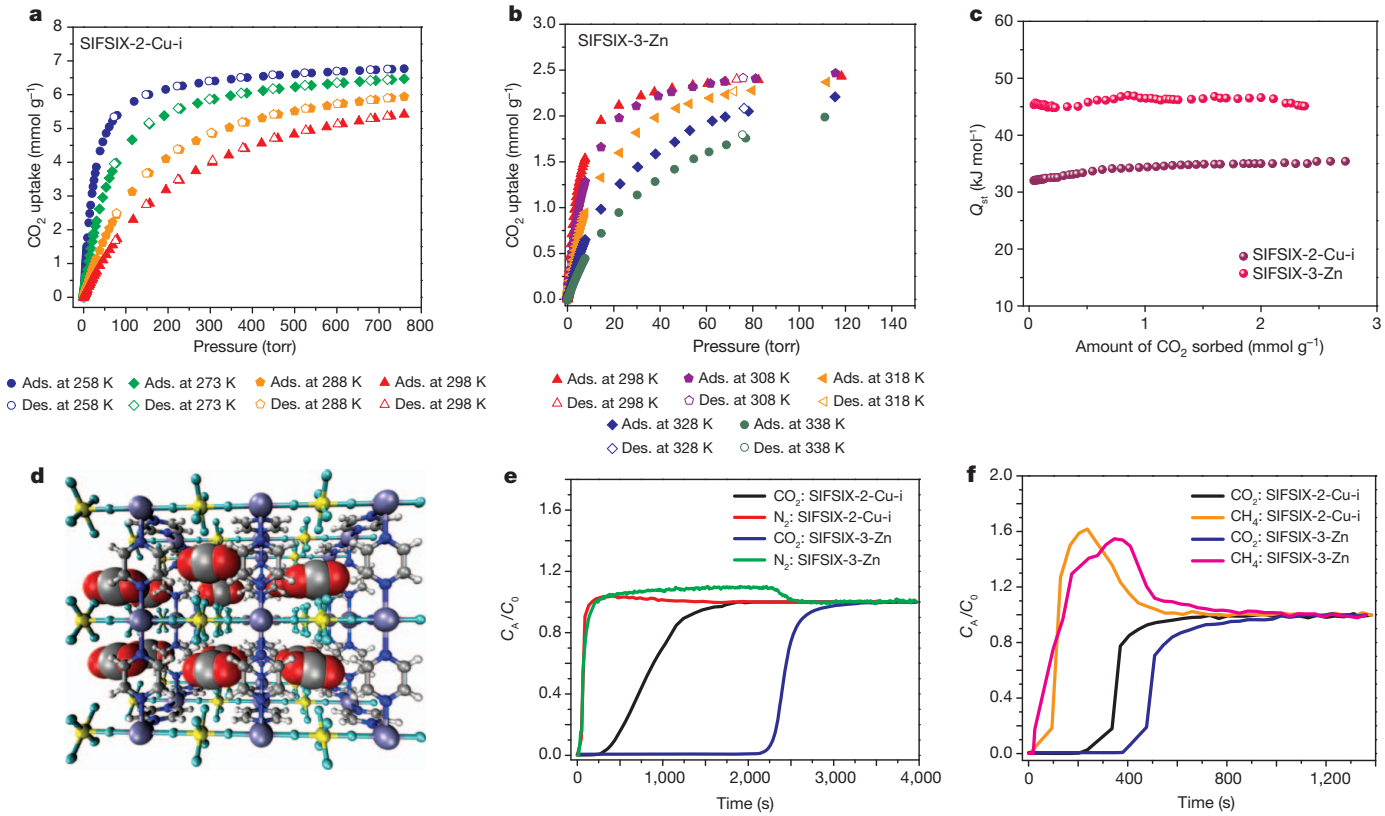

Figure 2 | Pure gas adsorption, modelling and gas mixture breakthrough studies of SIFSIX compounds. **a**, **b**, Variable temperature CO_2 sorption isotherms for SIFSIX-2-Cu-i (**a**) and SIFSIX-3-Zn (**b**). **c**, Q_{st} of CO_2 adsorption on SIFSIX-2-Cu-i and SIFSIX-3-Zn in the low pressure region. **d**, The modelled structure of a $3 \times 3 \times 3$ box of unit cells of SIFSIX-3-Zn reveals close interactions between the electropositive carbon atoms of CO_2 molecules and fluorine atoms of SIFSIX anions. Colour code: C (grey), H (white), N (blue), O (red), Si (yellow), F (green), Zn (purple). **e**, Column breakthrough experiment for a CO_2/N_2:10/90 gas mixture (298 K, 1 bar) carried out on SIFSIX-2-Cu-i and SIFSIX-3-Zn. **f**, As **e** but for a CO_2/CH_4:50/50 gas mixture (298 K, 1 bar).

adsorption on SIFSIX-2-Cu-i reached a plateau at relatively higher pressures (5–7 bar) (Supplementary Fig. 9b). As a result, SIFSIX-3-Zn exhibits high volumetric CO_2 uptake that is comparable to those of Mg-dobdc (ref. 10) and UTSA-16 (ref. 25) at a CO_2 partial pressure typical for post-combustion CO_2 capture (Supplementary Fig. 23).

Figure 2c presents the Q_{st} of CO_2 adsorption for SIFSIX-2-Cu-i and SIFSIX-3-Zn from variable temperature isotherms (Fig. 2a, b), and the Q_{st} of up to 45 kJ mol^{-1} is consistent with the steepness of the CO_2 isotherms. The relatively constant Q_{st} indicates homogeneous binding sites over the full range of CO_2 loading (Fig. 2c). These Q_{st} values are in the 'sweet spot' favourable for efficient, reversible adsorption–desorption—that is, strong but still reversible—and are supported by modelling studies (Fig. 2d, Supplementary Figs 25–27).

The CO_2 selectivity of SIFSIX-3-Zn was investigated via column breakthrough tests using binary CO_2/N_2:10/90 (Fig. 2e) and CO_2/CH_4:50/50 gas mixtures (Fig. 2f) at 298 K and atmospheric pressure, and compared to the corresponding breakthrough tests on SIFSIX-2-Cu-i. Remarkably, SIFSIX-3-Zn showed much higher selectivity (495 and 109 for CO_2/N_2:10/90 and CO_2/CH_4:50/50, respectively) than SIFSIX-2-Cu-i, as CO_2 was retained for longer times (for example, ~2000 s versus 300 s for CO_2/N_2). Notably, N_2 and CH_4 breakthrough occurred within seconds, indicative of high selectivity toward CO_2. To support and confirm the high selectivity derived from the breakthrough experiments, single-gas (CO_2, N_2, CH_4 and H_2) sorption isotherms were measured at low and high pressures and IAST calculations were used to predict adsorption equilibria for the following binary mixtures: CO_2/CH_4:05/95, CO_2/CH_4:50/50, CO_2/N_2:10/90 and CO_2/H_2:30/70. These mixtures mimic natural gas upgrading, biogas treatment, and post- and pre-combustion capture applications, respectively.

Figure 3a and b shows that the CO_2 adsorption selectivity of SIFSIX-3-Zn calculated for binary gas separation versus CH_4 and N_2 is unprecedented, outperforming Mg-dobdc (ref. 10), UTSA-16 (ref. 25) and zeolite 13X (ref. 26). Indeed, the selectivity of SIFSIX-3-Zn is comparable to that of amine-functionalized MOFs[27] and amine-bearing mesoporous silica[28], particularly at low CO_2 partial pressure. The calculated selectivity for CO_2/N_2 (that is, 1,539 ± 307 at 1 bar and 298 K) was validated by gas mixture gravimetric adsorption experiments at various pressures (Fig. 3c, d).

With regards to CO_2/H_2 mixtures, adsorption isotherms of CO_2/H_2:30/70 were collected and showed similar shapes and uptakes to that obtained using pure CO_2 (Supplementary Fig. 10). This indicates that SIFSIX-3-Zn adsorbs CO_2 with very large selectivity over H_2 (higher than 1,800), making it potentially suitable for pre-combustion capture or H_2 purification. Because of the large error associated with H_2 adsorption measurement (due to the relatively low uptake), quantitative measurements of CO_2/H_2 selectivity were not possible. We note that calculated and measured selectivities exceeding 1,000 are often subject to uncertainties associated with measurement of the uptake of weakly adsorbed gases. Therefore, it would be inappropriate in this case to make quantitative comparisons between different adsorbents such as SIFSIX-3-Zn and Mg-dobdc[29] (800 at 1 bar and 313 K).

To confirm the synergistic nature of the thermodynamics and kinetics for CO_2 capture, competitive adsorption kinetic studies of the above gas mixtures were conducted and are presented in Fig. 3e. We note that the CO_2 non-equilibrium uptake at equal times for CO_2/N_2, CO_2/CH_4 and CO_2/H_2 mixtures follows the behaviour of pure CO_2. In addition, at equilibrium the total CO_2 uptake from the CO_2-containing gas mixtures agrees perfectly with the equilibrium uptake for pure CO_2. These distinctive findings show that when CO_2-containing mixtures are in contact with SIFSIX-3-Zn, CO_2 adsorbs more strongly and faster than N_2, O_2, CH_4 and H_2, thus occupying all the available space and sorption sites and consequently excluding other gases. Most

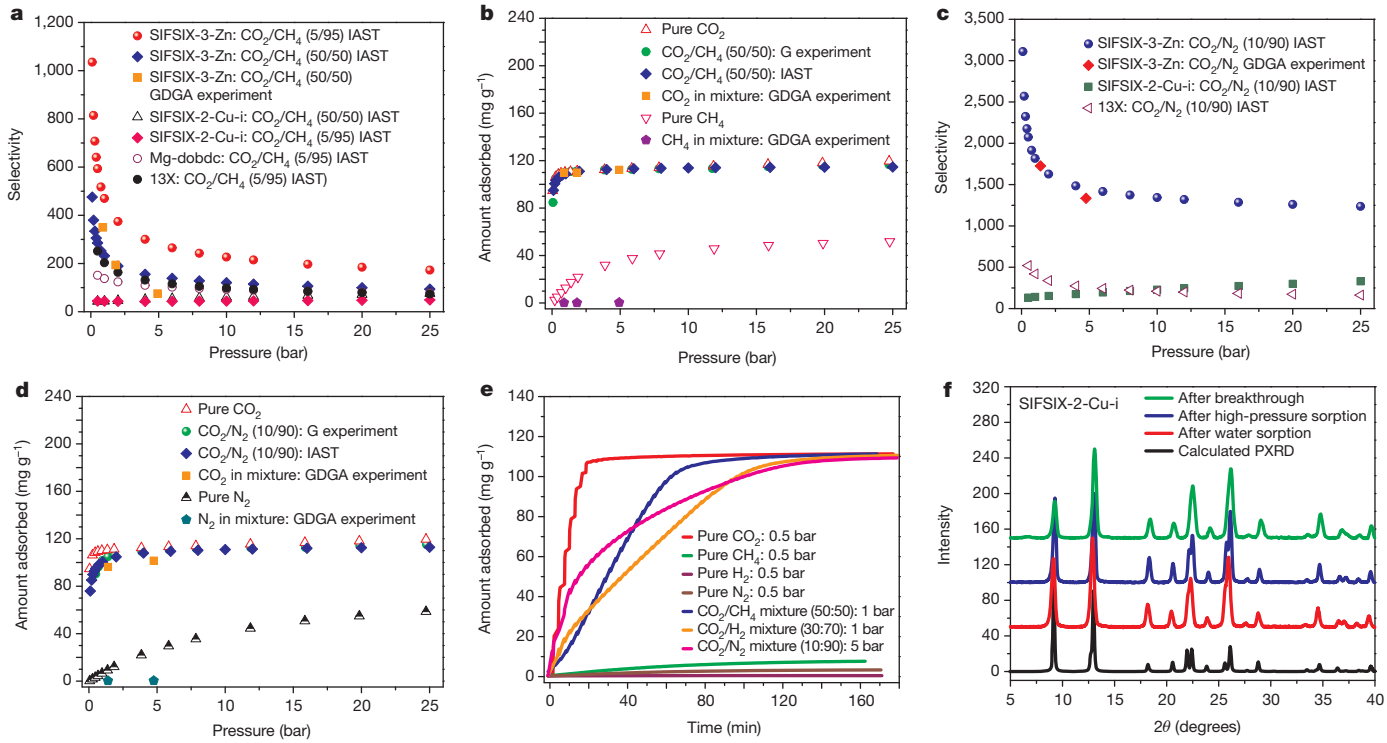

Figure 3 | Gas mixture selectivity of SIFSIX compounds and the stability study of SIFSIX-2-Cu-i. **a**, Calculated (using IAST) CO_2 adsorption selectivity for two different CO_2/CH_4 mixtures on SIFSIX-2-Cu-i and SIFSIX-3-Zn compared to Mg-dobdc and 13X zeolite at 298 K. Experimental data using gravimetric-densimetric gas analysis (GDGA) are provided for comparison. **b**, IAST CO_2/CH_4:50:50 adsorption isotherm prediction compared to experimental pure CO_2, CH_4 and CO_2/CH_4:50:50 gas mixture adsorption isotherms collected using gravimetric (G) adsorption experiments for SIFSIX-3-Zn at 298 K. **c**, CO_2 adsorption selectivity of SIFSIX-2-Cu-i, SIFSIX-3-Zn and 13X zeolite for CO_2/N_2:10:90 as calculated using IAST at 298 K. **d**, IAST CO_2/N_2:10:90 adsorption isotherm predictions compared to experimental pure CO_2, N_2 and CO_2/N_2:10:90 gas mixture adsorption isotherms collected using gravimetric (G) adsorption experiments for SIFSIX-3-Zn at 298 K. **e**, Kinetics of adsorption of SIFSIX-3-Zn for pure gases and gas mixtures containing various compositions of CO_2. **f**, PXRD patterns of SIFSIX-2-Cu-i after multiple cycles of breakthrough tests, high-pressure sorption, and water sorption experiments (compared to the calculated pattern).

importantly, SIFSIX-3-Zn fulfils the demanding attributes (Supplementary Fig. 7) required for economical and efficient CO_2 post-combustion separation. Further, increasing the adsorption temperature did not significantly reduce the steepness of the CO_2 adsorption isotherm for SIFSIX-3-Zn (Fig. 2b, Supplementary Fig. 8); this is a desirable feature in many CO_2 separation and purification applications.

Whereas the sorbents reported here exhibit very good performance with respect to CO_2 selectivity, their amenability to recycling and efficacy in the presence of moisture must also be addressed. The former was validated via adsorption–desorption cycle experiments conducted at 323 K and 0.15 bar (Supplementary Fig. 14). The latter—specifically, the effect of water vapour on the CO_2 capacity and selectivity of SIFSIX-2-Cu-i and SIFSIX-3-Zn—was evaluated via a series of adsorption measurements. The water vapour adsorption isotherms are found to be of type I, with uptakes of 20 wt% and 11 wt%, respectively, at 74% relative humidity (Supplementary Fig. 24). Water adsorption affinity/capacity is reduced in the presence of CO_2 gas mixtures, as shown by breakthrough experiments, especially for SIFSIX-3-Zn (Supplementary Figs 15b and 16b). Importantly, the presence of water in the given gas mixture had a negligible effect at elevated CO_2 concentrations (Supplementary Fig. 15) in the case of SIFSIX-2-Cu-i. Regarding the CO_2/H_2:30/70 mixture, CO_2 uptake and selectivity were only slightly reduced in the presence of moisture (1.61 mmol g^{-1} and 191 at 74% relative humidity versus 1.99 mmol g^{-1} and 237 at 0% relative humidity for SIFSIX-2-Cu-i, Supplementary Fig. 15b). Whereas SIFSIX-2-Cu-i was structurally unchanged by exposure to moisture (Fig. 3f), SIFSIX-3-Zn undergoes a reversible phase change at relatively high humidity (Supplementary Figs 19–22).

We have demonstrated how a crystal engineering or reticular chemistry approach to pore size control, coupled with favourable electrostatic interactions provided by an array of inorganic anions, affords porous materials with exceptional selectivity, recyclability and moisture stability in the context of several industrially relevant CO_2 separation applications. The structural features and exceptional mixed-gas sorption properties of the SIFSIX compounds reported here show that it is now possible to combine equilibrium[10,11,26] and kinetic[30] adsorption selectivity in the same porous material to facilitate effective CO_2 separation and capture.

Received 3 July; accepted 20 December 2012.
Published online 27 February 2013.

1. Taylor, P. *Energy Technology Perspectives 2010 — Scenarios and Strategies to 2050* 74 (International Energy Agency, Paris, 2010).
2. Merel, J., Clausse, M. & Meunier, F. Experimental investigation on CO_2 post-combustion capture by indirect thermal swing adsorption using 13X and 5A zeolites. *Ind. Eng. Chem. Res.* **47,** 209–215 (2008).
3. MacGillivray, L. R. *Metal-Organic Frameworks: Design and Application* (Wiley & Sons, 2010).
4. Li, H., Eddaoudi, M., O'Keeffe, M. & Yaghi, O. M. Design and synthesis of an exceptionally stable and highly porous metal-organic framework. *Nature* **402,** 276–279 (1999).
5. Eddaoudi, M. *et al.* Systematic design of pore size and functionality in isoreticular MOFs and their application in methane storage. *Science* **295,** 469–472 (2002).
6. Farha, O. K. *et al.* Metal–organic framework materials with ultrahigh surface areas: is the sky the limit? *J. Am. Chem. Soc.* **134,** 15016–15021 (2012).
7. Moulton, B. & Zaworotko, M. J. From molecules to crystal engineering: supramolecular isomerism and polymorphism in network solids. *Chem. Rev.* **101,** 1629–1658 (2001).
8. Kitagawa, S., Kitaura, R. & Noro, S. Functional porous coordination polymers. *Angew. Chem. Int. Edn* **43,** 2334–2375 (2004).
9. Yaghi, O. M. *et al.* Reticular synthesis and the design of new materials. *Nature* **423,** 705–714 (2003).
10. Caskey, S. R., Wong Foy, A. G. & Matzger, A. J. Dramatic tuning of carbon dioxide uptake via metal substitution in a coordination polymer with cylindrical pores. *J. Am. Chem. Soc.* **130,** 10870–10871 (2008).

11. Sumida, K. *et al.* Carbon dioxide capture in metal–organic frameworks. *Chem. Rev.* **112,** 724–781 (2012).
12. Kizzie, A. C., Wong Foy, A. G. & Matzger, A. J. Effect of humidity on the performance of microporous coordination polymers as adsorbents for CO_2 capture. *Langmuir* **27,** 6368–6373 (2011).
13. Subramanian, S. & Zaworotko, M. J. Porous solids by design — $[Zn(4,4'\text{-}bpy)_2(SiF_6)_n]$-xDMF, a single framework octahedral coordination polymer with large square channels. *Angew. Chem. Int. Edn* **34,** 2127–2129 (1995).
14. Noro, S., Kitagawa, S., Kondo, M. & Seki, K. A new methane adsorbent, porous coordination polymer $[CuSiF_6(4,4'\text{-bipyridine})_2]_n$. *Angew. Chem. Int. Edn* **39,** 2081–2084 (2000).
15. Burd, S. D. *et al.* Highly selective carbon dioxide uptake by $[Cu(bpy\text{-}n)_2(SiF_6)]$ (bpy-1 = 4,4′-bipyridine; bpy-2 = 1,2-bis(4-pyridyl)ethene). *J. Am. Chem. Soc.* **134,** 3663–3666 (2012).
16. Coe, B. J. *et al.* Syntheses, spectroscopic and molecular quadratic nonlinear optical properties of dipolar ruthenium(II) complexes of the ligand 1,2-phenylenebis(dimethylarsine). *Dalton Trans.* (18), 2935–2942 (2004).
17. Uemura, K., Maeda, A., Maji, T. K., Kanoo, P. & Kita, H. Syntheses, crystal structures and adsorption properties of ultramicroporous coordination polymers constructed from hexafluorosilicate ions and pyrazine. *Eur. J. Inorg. Chem.* (16), 2329–2337 (2009).
18. Jagiello, J. & Thommes, M. Comparison of DFT characterization methods based on N_2, Ar, CO_2, and H_2 adsorption applied to carbons with various pore size distributions. *Carbon* **42,** 1227–1232 (2004).
19. Ma, S. *et al.* Framework-catenation isomerism in metal−organic frameworks and its impact on hydrogen uptake. *J. Am. Chem. Soc.* **129,** 1858–1859 (2007).
20. Llewellyn, P. L. *et al.* High uptakes of CO_2 and CH_4 in mesoporous metal-organic frameworks MIL-100 and MIL-101. *Langmuir* **24,** 7245–7250 (2008).
21. Lässig, D. *et al.* A microporous copper metal–organic framework with high H_2 and CO_2 adsorption capacity at ambient pressure. *Angew. Chem. Int. Edn* **123,** 10528–10532 (2011).
22. Yazaydın, A. O. *et al.* Enhanced CO_2 adsorption in metal-organic frameworks via occupation of open-metal sites by coordinated water molecules. *Chem. Mater.* **21,** 1425–1430 (2009).
23. Myers, A. L. & Prausnitz, J. M. Thermodynamics of mixed-gas adsorption. *Am. Inst. Chem. Eng. J.* **11,** 121–127 (1965).
24. Ho, M. T., Allinson, G. W. & Wiley, D. E. Reducing the cost of CO_2 capture from flue gases using pressure swing adsorption. *Ind. Eng. Chem. Res.* **47,** 4883–4890 (2008).
25. Xiang, S. *et al.* Microporous metal-organic framework with potential for carbon dioxide capture at ambient conditions. *Nature Commun.* **3,** 954 (2012).
26. Cavenati, S., Grande, C. A. & Rodrigues, A. E. Adsorption equilibrium of methane, carbon dioxide, and nitrogen on zeolite 13X at high pressures. *J. Chem. Eng. Data* **49,** 1095–1101 (2004).
27. Vaidhyanathan, R. *et al.* Direct observation and quantification of CO_2 binding within an amine-functionalized nanoporous solid. *Science* **330,** 650–653 (2010).
28. Belmabkhout, Y., Serna-Guerrero, R. & Sayari, A. Adsorption of CO_2-containing gas mixtures over amine-bearing pore-expanded MCM-41 silica: application for gas purification. *Ind. Eng. Chem. Res.* **49,** 359–365 (2010).
29. Herm, Z. R., Swisher, J. A., Smit, B., Krishna, R. & Long, J. R. Metal-organic frameworks as adsorbents for hydrogen purification and precombustion carbon dioxide capture. *J. Am. Chem. Soc.* **133,** 5664–5667 (2011).
30. Han, S. *et al.* High-throughput screening of metal–organic frameworks for CO_2 separation. *ACS Combinat. Sci.* **14,** 263–267 (2012).

Supplementary Information is available in the online version of the paper.

Acknowledgements This publication is based on work supported by KAUST award number FIC/2010/06 (M.E. and M.J.Z.) and KAUST start up funds (M.E.). B.S. acknowledges computational resources made available by an XSEDE grant (number TG-DMR090028). Single-crystal diffraction experiments on SIFSIX-2-Cu-i were conducted at the Advanced Photon Source on beamline 15ID-B of ChemMatCARS Sector 15, which is principally supported by the National Science Foundation/ Department of Energy under grant number NSF/CHE-0822838. Use of the Advanced Photon Source was supported by the US Department of Energy, Office of Science, Office of Basic Energy Sciences under contract number DE-AC02-06CH11357.

Author Contributions P.N., S.D.B. and M.J.Z. contributed to the conceptual approach to designing the materials synthetic experiments; P.N. and S.D.B. carried out the materials synthesis ; L.W. and R.L. conducted and interpreted the crystallographic experiments; P.N., S.D.B., Y.B., S.M., M.E. and A.J.C. conducted and interpreted low-pressure sorption experiments; Y.B. and M.E. contributed to the initial ideas, conceptualizing, designing, conducting (Y.B.) and interpreting sorption experiments for gas separation of various industrially relevant gas mixtures (high-pressure single and mixed gas sorption experiments, sorption kinetics and breakthrough experiments) and IAST calculations; K.F., T.P. and B.S. conducted electrostatic models of gas sorption; and M.E. and M.J.Z. wrote the manuscript.

Author Information Supplementary crystallographic data for this manuscript has been deposited at the Cambridge Crystallographic Data Centre under deposition numbers CCDC 914600 and 914601. These data can be obtained free of charge from http://www.ccdc.cam.ac.uk/data_request/cif. Reprints and permissions information is available at www.nature.com/reprints. The authors declare no competing financial interests. Readers are welcome to comment on the online version of the paper. Correspondence and requests for materials should be addressed to M.E. (mohamed.eddaoudi@kaust.edu.sa) and M.J.Z. (xtal@usf.edu).